

# Molecular interactions in bacterial cellulose composites studied by 1D FT-IR and dynamic 2D FT-IR spectroscopy

Marta Kačuráková,<sup>a</sup> Andrew C. Smith,<sup>a</sup> Michael J. Gidley,<sup>b</sup> Reginald H. Wilson<sup>a,\*</sup>

<sup>a</sup>Norwich Laboratory, Institute of Food Research, Norwich Research Park, Colney Lane, Norwich NR4 7UA, UK

<sup>b</sup>Unilever Research, Colworth House, Sharnbrook, Bedford MK44 1LQ, UK

Received 19 July 2001; received in revised form 21 March 2002; accepted 10 April 2002

## Abstract

Specific strain-induced orientation and interactions in three *Acetobacter* cellulose composites: cellulose (C), cellulose/pectin (CP) and cellulose/xyloglucan (CXG) were characterized by FT-IR and dynamic 2D FT-IR spectroscopies. On the molecular level, the reorientation of the cellulose fibrils occurred in the direction of the applied mechanical strain. The cellulose-network reorientation depends on the composition of the matrix, including the water content, which lubricates the motion of macromolecules in the network. At the submolecular level, dynamic 2D FT-IR data suggested that there was no interaction between cellulose and pectin in CP and that they responded independently to a small amplitude strain, while in CXG, cellulose and xyloglucan were uniformly strained along the sample length. © 2002 Elsevier Science Ltd. All rights reserved.

**Keywords:** Cellulose composites; FT-IR spectroscopy; Dynamic 2D FT-IR spectroscopy; Linear stretching

## 1. Introduction

Cellulose is composed of  $\beta$ -D-glucopyranose units joined by (1 $\rightarrow$ 4)-glycosidic links, and is the primary structural element of the cell wall: it has a high molecular weight and crystallinity.<sup>1</sup> Xyloglucan is the major hemicellulose component in primary cell walls, with chains of (1 $\rightarrow$ 4)- $\beta$ -D-glucan with xylosyl units linked to the glucosyl units in the C-6 position. Pectin is a term for a group of heterogeneous polysaccharides whose backbone consists of (1 $\rightarrow$ 4)-linked  $\alpha$ -D-galacturonic acid repeating-units. Bacterial (*Acetobacter xylinum*) cellulose-based composites containing xyloglucan or pectin have been shown to possess organizational features similar to those observed in primary plant cell walls.<sup>2–4</sup>

Infrared (IR) spectroscopy has been extensively used in cellulose research and IR band assignment, orientation data,<sup>5,6</sup> and structural details<sup>7,8</sup> have been produced. Polymer stiffness is considerably enhanced by molecular orientation, and polarized IR spectroscopy

can be used to study orientation induced by mechanical strain and to characterize the segmental mobility of polymers under the influence of an external perturbation.<sup>9</sup> Dynamic 2D FT-IR spectroscopy has been used to unravel the IR bands affected by deformation and the orientation of submolecular groups in cellulose I in order to probe the relationship between hydrogen bonding and cellulose structure<sup>10–12</sup> in dry spruce-pulp samples. We have recently reported the first application of linear stretching FT-IR microscopy and 2D FT-IR spectroscopy<sup>13</sup> to functional cell walls in onion epidermis. However, it is necessary to determine the 2D cross-correlation peak frequencies for pure cellulose and its composites with other cell-wall biopolymers in order to establish an interpretation of cross peaks in hydrated systems.

Here we report the results of an FT-IR study of mechanically strained hydrated cellulose composites and interpret the data in terms of molecular mobility and interactions. Well-characterized model systems were used for detailed studies to allow interpretations to be applied to polymers of intact plant cell walls. Polarized IR spectra allow the determination of molecular alignment and contribute towards an understanding of the structure–function relationship in biopoly-

\* Corresponding author. Tel.: +44-1603-255000.

E-mail address: [reg.wilson@bbsrc.ac.uk](mailto:reg.wilson@bbsrc.ac.uk) (R.H. Wilson).

mer mixtures at different water contents. The analysis of the dynamic 2D FT-IR spectra and two-dimensional correlations are shown for samples measured with a polarized IR source.

## 2. Experimental

**Materials.**—The *Acetobacter* cellulose samples cellulose (C), cellulose/pectin (CP, containing 20% apple pectin of 67% degree of methyl esterification), and cellulose/xyloglucan (CXG, containing 35% of tamarind xyloglucan) were prepared as described previously.<sup>2–4</sup> Fermentation duration of 24 h gave 10–20  $\mu\text{m}$  thick films, which were still measurable with IR absorbance up to about 2 units in transmission, yet strong enough to be mounted in the clamps of the stretching device. The weight fraction of different cellulose morphologies in the C and CP samples has been reported as 57% I $\alpha$ , 25% I $\beta$  crystalline, and 18% non-crystalline,<sup>4</sup> while in CXG the corresponding values were 21% I $\alpha$ , 32% I $\beta$  crystalline, and 47% non-crystalline.<sup>2,3</sup>

**Water content.**—The water content was gravimetrically determined after the cellulose composites were equilibrated at discrete relative humidity (RH) values.<sup>13</sup> The samples at 100% relative humidity (RH) showed (Table 1) water contents (w/w) of: 42% for C, 61% for CP, and 94% for CXG. Samples used for dynamic 2D and linear stretching experiments were measured at 97% RH (defined as wet samples, w-samples) and certain samples were measured after partial drying at 84% RH (defined as moist, m-samples) as shown in Table 1. Samples dried below 76% RH were effectively dry, brittle, and not suitable for FT-IR mechanical investigation.

**FT-IR spectroscopy.**—A Bio-Rad FTS 6000 (Cambridge, MA) spectrometer, equipped with a liquid nitrogen cooled MCT (HgCdTe) detector, was used to collect transmission spectra. In linear stretching exper-

iments, 128 scans were co-added before Fourier transformation with the IR beam polarized parallel or perpendicular to the stretching direction using a KRS 5 (TlBr and TlI mixed crystal) wire-grid polarizer (Graseby Specac, UK). The resolution was 8  $\text{cm}^{-1}$  and three to five replicates were measured in order to ensure reproducibility of measurement. The spectrometer was controlled by a computer running WIN-IR PRO (Bio-Rad) version 2.9.

**Linear stretching.**—Polarized FT-IR spectra were collected from oriented samples. The composite samples were washed in water, cut to  $\sim 15 \times 10$  mm and mounted between the jaws of a Bio-Rad polymer stretcher. The sample was stretched ( $\Delta l$  is the change of length) in steps of 3% strain,  $\epsilon$ , ( $\Delta l/l$ ) from 0 to 33%.

**Infrared dichroism.**—Infrared dichroism reflects the mean orientation of the transition moments of the corresponding vibrational modes. Anisotropy following an applied deformation is characterized by the *dichroic difference*  $\Delta A = (A_{\parallel} - A_{\perp})$  and/or *dichroic ratio* defined as  $R = A_{\parallel}/A_{\perp}$ , where the  $A_{\parallel}$  and  $A_{\perp}$  are the absorbances measured with parallel and perpendicular polarization.<sup>14–16</sup> The cellulose composites were studied as a function of uniaxial strain. For a polymer network, the segmental orientation ( $F$ ) detected by IR spectroscopy<sup>17</sup> expressed in terms of the dichroic ratio is:  $F = C[(R - 1)/(R + 2)]$ , where  $C = (2 \cot^2 \alpha + 2)/(2 \cot^2 \alpha - 1)$ . For a given absorption band,  $\alpha$  is the angle between the transition moment vector of the vibrational mode and a directional vector characteristic of the chain segment. The glycosidic (C–O–C) link (band at 1162  $\text{cm}^{-1}$ ) is approximately co-aligned with the molecular long axis<sup>1,6</sup> and the stretching direction. In this case,  $\alpha = 0^\circ$  and the equation reduces to:  $F = (R - 1)/(R + 2)$ .

**Data analysis.**—In order to analyze the strain-induced IR spectral changes,  $\Delta A$  and  $F$  of selected bands were used to characterize the degree of orientation of cellulose in the individual composites<sup>9,14,17</sup> in correlation with uniaxial strain. One of the effects of stretching is a change in the thickness of the polymer film. In order to minimize resultant error in  $\Delta A$ , each polarized spectrum was normalized to the corresponding unstretched IR absorption in the  $\delta(\text{CH})$  region at (1400–1300  $\text{cm}^{-1}$ ) where intensity is not orientation dependent.<sup>18</sup> For molecular orientation analysis  $\Delta A$  was used, in which case the bands from vibrational dipoles parallel to the polymer-chain axis appeared with positive intensity, whereas those that are perpendicular were of negative intensity.<sup>15</sup>

**Dynamic 2D FT-IR spectroscopy.**—In dynamic 2D FT-IR, a small-amplitude oscillatory strain is applied to a sample and the resulting spectral changes are measured as a function of time.<sup>13</sup> The dynamic perturbation generates directional changes in the transi-

Table 1  
Sorption isotherm data

Relative humidity (%)	C	CP	CXG	Samples
100	42	61	94	
97	30	56	87	w
95	28	40	79	
84	22	20	12	m
76	18	10	2	

Water content (w/w%) in the cellulose composite samples: cellulose (C), cellulose/pectin (CP) and cellulose/xyloglucan (CXG).

Table 2

Assignment and orientation of cellulose, pectin and xyloglucan FT-IR absorption bands <sup>a</sup> as they were observed in the cellulose composites

Frequency (cm <sup>-1</sup> )	Assignment	Bond, orientation	Origin
1740	$\nu(\text{C=O})$		ester, <b>P</b>
1426	$\delta_s\text{CH}_2$		<b>C</b>
1371	$\delta\text{CH}_2\text{w}$		<b>XG</b>
1362, 1317	$\delta_s\text{CH}_2\text{w}$	$\perp$	<b>C</b>
1243	$\nu(\text{C-O})$		<b>P</b>
1160	$\nu_{\text{as}}(\text{C-O-C})$	glycosidic link, ring, $\parallel$	
1146	$\nu_{\text{as}}(\text{C-O-C})$	glycosidic link, ring, $\parallel$	<b>P</b>
1130	$\nu_{\text{as}}(\text{C-O-C})$	glycosidic link, ring, $\parallel$	<b>XG</b>
1115	$\nu(\text{C-O}), \nu(\text{C-C})$	C-2-O-2	<b>C</b>
1100	$\nu(\text{C-O}), \nu(\text{C-C})$	ring	<b>P</b>
1075	$\nu(\text{C-O}), \nu(\text{C-C})$	ring	<b>XG</b>
1060	$\nu(\text{C-O}), \nu(\text{C-C})$	C-3-O-3, $\parallel$	
1042	$\nu(\text{C-O}), \nu(\text{C-C})$	ring,	<b>XG</b>
1030	$\nu(\text{C-O}), \nu(\text{C-C})$	C-6-H <sub>2</sub> -O-6, $\parallel$	
1015, 1000	$\nu(\text{C-O}), \nu(\text{C-C})$	C-6-H <sub>2</sub> -O-6, $\parallel$	<b>C</b>
1019	$\nu(\text{C-O}), \nu(\text{C-C})$	C-2-C-3, C-2-O-2, C-1-O-1	<b>P</b>
960	$\delta(\text{CO})$	$\parallel$	<b>P</b>
944	ring	$\parallel$	<b>XG</b>
895	$\delta(\text{C-1-H})$	$\beta$ -anomeric link	<b>C, XG</b>
833	ring	$\parallel$	<b>P</b>

Key: IR vibrations:  $\nu$ , stretching;  $\delta$ , bending; w, wagging; <sub>s</sub> symmetric; <sub>as</sub> asymmetric; **C**, cellulose; **P**, pectin; **XG**, xyloglucan;  $\parallel$ , parallel;  $\perp$ , perpendicular orientation.

<sup>a</sup> IR band assignment is based on literature using Refs. 5,6,13,21,22.

tion moments of functional groups whose relaxations then depend upon inter- and intramolecular couplings. The resulting dynamic absorbance spectra, which vary sinusoidally with the stretching frequency, are deconvoluted into two separate spectra: the in-phase (IP) spectrum reveals the re-orientational motions of electrical dipole moments occurring simultaneously, and the quadrature (Q) spectrum those which are  $\pi/2$  out-of-phase with respect to the applied strain. From the IP and Q spectra, synchronous 2D correlation spectra can be obtained with correlation peaks at wavenumber coordinates where the IR signal responses are in-phase with each other.<sup>16,19,20</sup>

Dynamic 2D FT-IR spectra were measured on samples ( $\sim 15 \times 10$  mm) mounted in a Bio-Rad polymer stretcher and pre-stretched to 21% strain. The spectra were acquired on a BioRad FTS 6000 equipped with an MCT detector. The IR beam was polarized parallel or perpendicular to the direction of stretch using a KRS 5 wire-grid polarizer. Sample modulation frequencies (SMF) of 5, 10, 16, 20, 25, and 50 Hz, were used with an amplitude of 100  $\mu\text{m}$ . Two scans at resolution 8  $\text{cm}^{-1}$  were co-added and the IP and Q spectra were ratioed to the static spectra. 2D correlation spectra were constructed using MATLAB software, version 6.0 from the IP and Q spectra using cross-correlation analysis.<sup>20</sup>

### 3. Results and discussion

Linear stretching experiments were performed to examine the changes in infrared absorption spectra of samples with applied uniaxial strain. From the polarized FT-IR spectra, dichroic difference,  $\Delta A$ , was calculated to evaluate the fibril reorientation, and dichroic ratio,  $R$ , was used to calculate the segmental orientation,  $F$ , of cellulose in order to compare the cellulose orientation as a function of strain in the different composites. Dynamic 2D FT-IR small-amplitude oscillatory strain was applied to the samples to study the inter- and intramolecular couplings at the sub-molecular level.

**1D FT-IR, transmission spectroscopy.**—The FT-IR spectral band assignments based on literature data are listed in Table 2. The absorption spectra of the cellulose composites **C**, **CP**, and **CXG** showed sharp IR bands across the whole 4000–800  $\text{cm}^{-1}$  region (Fig. 1). The intense absorption and high cellulose content compared to that of xyloglucan or pectin caused the **CP** and **CXG** spectra to be dominated by cellulose bands. In **CP** and **CXG** spectra the non-cellulose polymers could not easily be distinguished, but in **CP**, pectin bands were observed at 1738 and 833  $\text{cm}^{-1}$  and in **CXG** xyloglucan bands were seen at 1371 and 1317  $\text{cm}^{-1}$  with the anomeric band at 897  $\text{cm}^{-1}$  more intense than in pure

**C** due to the contribution from  $\beta$ -linked xyloglucan (Fig. 1). In the **CP** spectrum after subtraction of **C**, bands at 1738, 1243, 1146, 1097, 1019, 960, and 833  $\text{cm}^{-1}$  were seen, consistent with pectin<sup>21</sup> and in the **CXG** spectrum after subtraction of **C**, shoulders at 1130, 1079, 1045, and 944  $\text{cm}^{-1}$  corresponding to xyloglucan bands<sup>22</sup> (Table 2) were observed.

**Linear stretching and dichroic spectra. Wet samples.**—Linear stretching was first performed at the highest measurable water content (about 97% RH, Table 1) on cellulose (**C<sub>w</sub>**), cellulose/pectin (**CP<sub>w</sub>**), and cellulose/xyloglucan (**CXG<sub>w</sub>**) samples (where subscript w denotes wet samples). The unstretched samples showed very small or zero  $\Delta A$  across the entire spectrum. Dichroism of the cellulosic  $\nu_{\text{as}}(\text{C}-1-\text{O}-\text{C}-4)$  glycosidic link mode at 1162  $\text{cm}^{-1}$  was used as a measure of orientation.<sup>6,23</sup> Increased dichroism in the parallel direction was observed with increasing strain (Fig. 2(a)), indicating that the polymer aligned along the direction of stretch. The bands at 1058 and 1033  $\text{cm}^{-1}$  in **C<sub>w</sub>**, assigned to vibrations of C-3-H-O-3-H and C-6-H<sub>2</sub>-O-6-H cellulose groups and pyranosyl-ring vibrations,<sup>13</sup> increased in intensity without significant frequency shift. In **CP<sub>w</sub>** (Fig. 2(b)), the intensity at 1162  $\text{cm}^{-1}$  was much higher relative to the two-ring vibrations, which broadened, reflecting a wider distribution of the intra- and intermolecular hydrogen bond-energies compared to **C<sub>w</sub>**. In **CXG<sub>w</sub>**, the glycosidic 1062  $\text{cm}^{-1}$  band was the only one to show a significantly positive  $\Delta A$ , but relatively weak xyloglucan bands at 1075 and 1045  $\text{cm}^{-1}$  (Table 2) and also, frequency

shifts (Fig. 2(c)) in the 1070–1020  $\text{cm}^{-1}$  region were observed attributable to molecular deformation.<sup>16</sup>

**Moist samples.**—The samples designated **C<sub>m</sub>**, **CP<sub>m</sub>**, and **CXG<sub>m</sub>** were measured at 84% RH, where the subscript m denotes moist samples which contained only about 12–22% water (Table 1). In the m samples, the spectral features were similar to those for the w-series, but failure typically occurred at lower strain (18–21%). Therefore, water plays an important role in the deformation of the sample, consistent with the comment that the mechanical properties of these systems depend on hydration level.<sup>24</sup>

**Pre-stretched sample.**—An oriented (30% strain) **C<sub>w</sub>** sample was linearly stretched into a second dimension (**C<sub>ws</sub>**), perpendicular to the initial sample orientation. At the starting point of stretching the molecular orientation ( $\Delta A$ ) was observed to be perpendicular (Fig. 2(d)), but with increasing strain the negative bands at 1064, 1057, and 1037  $\text{cm}^{-1}$  tended to zero showing reorientation into the new stretching direction. This experiment demonstrated that the reorientation into the stretching direction occurs regardless of whether the initial orientation is random or partially orientated. The orientation is not perfect but it was certainly preferred.

**Orientation function.**—The orientation function ( $F$ ) of the cellulose glycosidic bond, a measure of distribution of cellulose chains segments, is shown as a function of strain in Fig. 3. Like  $\Delta A$ ,  $F$  increased<sup>17,25</sup> in all the samples but was generally larger for w-samples than for m-samples (Fig. 3). The enhanced ability of cellulose to orient in a wetter environment can be interpreted in

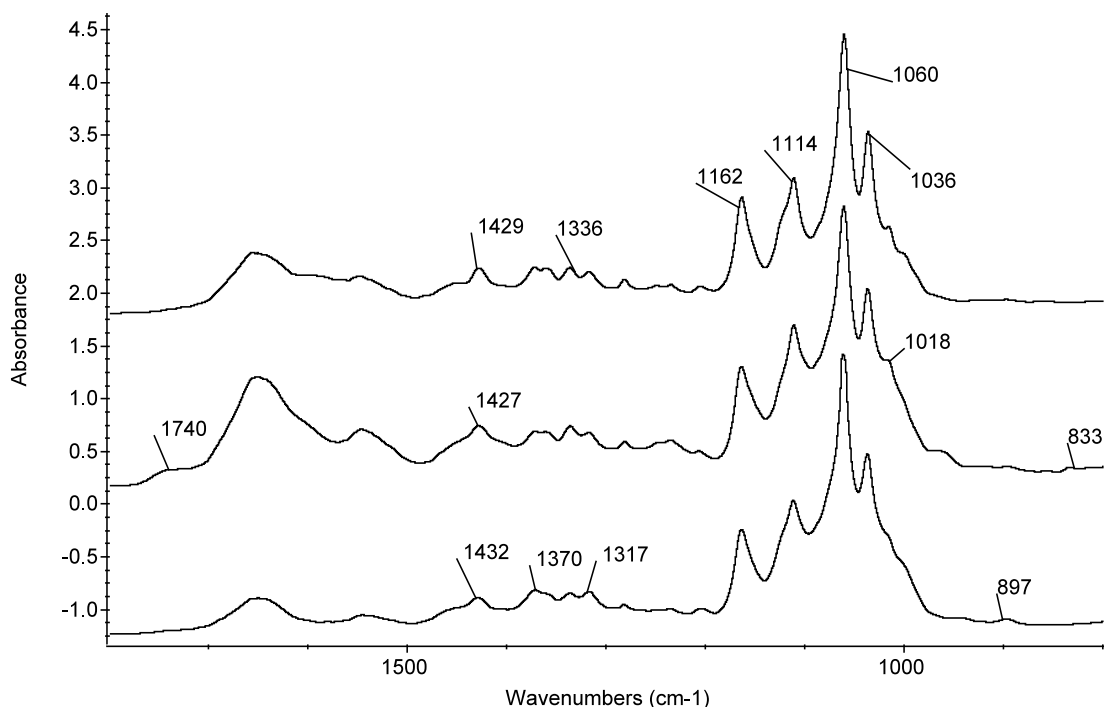


Fig. 1. FT-IR spectra of dry cellulose composites **C** (upmost), **CP** (centre), **CXG**.

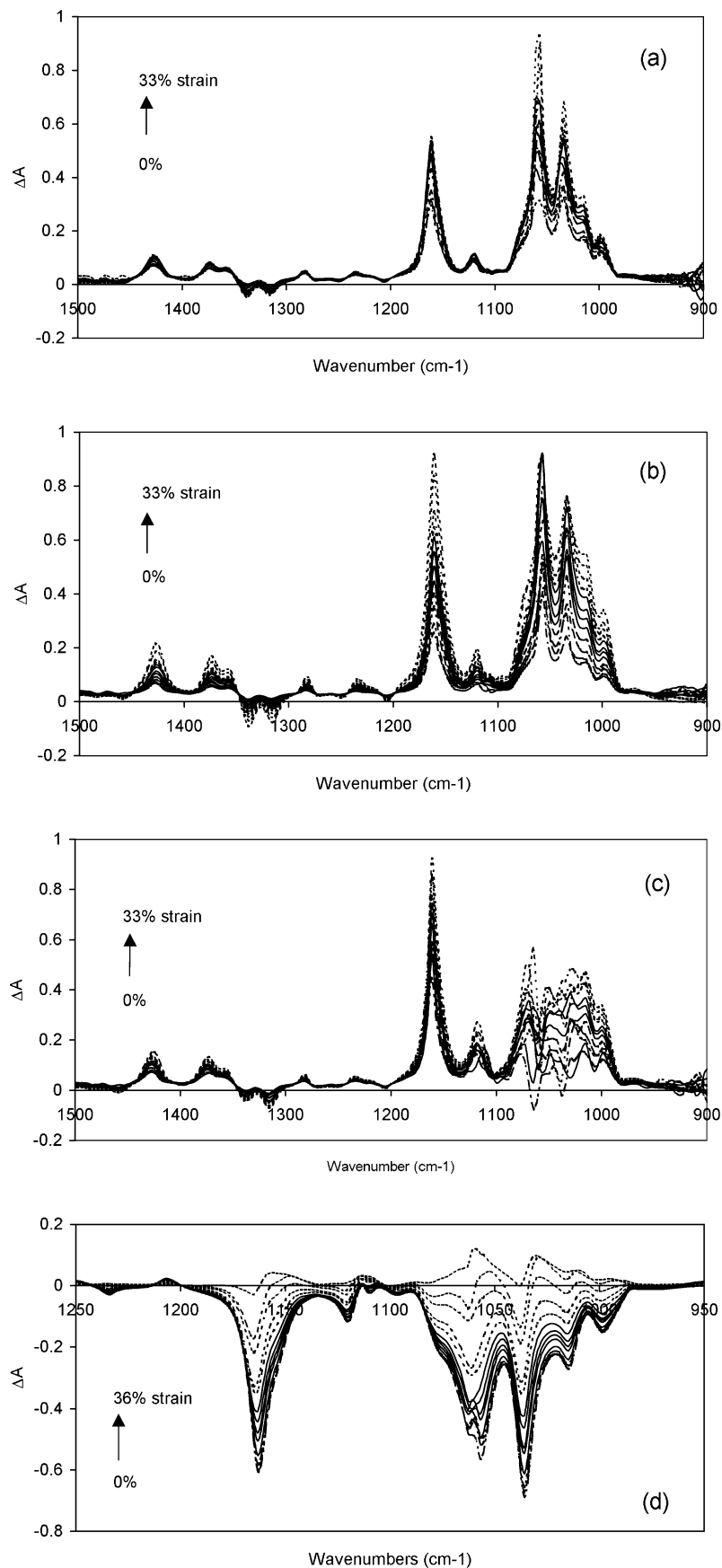


Fig. 2. Dichroic difference spectra ( $\Delta A = A_{||} - A_{\perp}$ ) taken from transmission FT-IR spectra, of wet,  $C_w$  (a),  $CP_w$  (b),  $CXG_w$  (c) cellulose composites and  $C_{ws}$  (d) oriented in second dimension; at each step of displacement with 3% steps. Bottom to top spectrum, strains: 0, 3, 6, 9 (···), 12, 15, 18, 21 (—), 24, 27, 30, 33, 36 (---)%.

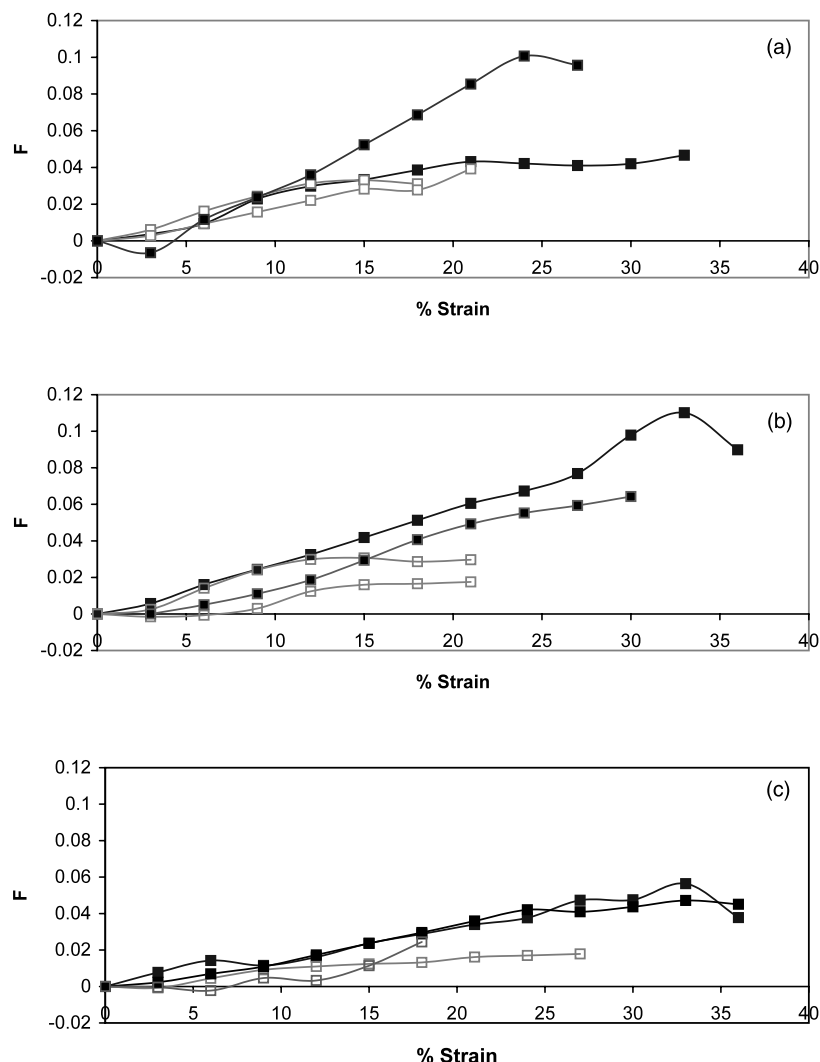


Fig. 3. Orientation function  $F$  of wet, w (■) and moist, m (□) composites:  $C_w$ ,  $C_m$  (a),  $CP_w$ ,  $CP_m$  (b), and  $CXG_w$ ,  $CXG_m$  (c), as a function of strain (%). Duplicates are shown.

terms of water lubricating the molecular motion within the fibrillar layers. In both the w- and m-samples,  $F$  for **CXG** was lower than for **C** and **CP**. In the original studies of these systems, the individual macromolecular networks may orient independently as a result of fewer fibril contacts<sup>4</sup> in **CP**, whereas in **CXG** the greater extensibility is related to alignment of cellulose in cross-linked cellulose–xyloglucan domains.<sup>3</sup> The orientation function (Fig. 3) showed that this network provides somewhat lower reorientation ability compared to **C** or **CP**. Whitney et al.<sup>3</sup> suggested that **C** contained a greater number of mechanically relevant interactions per unit volume, which are strained or broken upon elongation of the bulk material compared to **CXG**.

Recent small angle X-ray scattering (SAXS) results of strained composites<sup>24,26</sup> showed that the cellulose fiber orientation in all three composites **C**, **CP**, and **CXG** is similar. It is unclear whether this was due to a different sensitivity of FT-IR to molecular orientation

compared to SAXS or was simply due to the higher water content (95%) in the SAXS study, since water level has been shown to affect orientation (Fig. 3).

The FT-IR spectra (Fig. 2) showed that the fibrils in pure *Acetobacter* cellulose aligned in the longitudinal direction and the degree of alignment increased with increasing strain in accordance with observations in onion (*Allium cepa*).<sup>13</sup>

**Dynamic 2D FT-IR spectroscopy. Small amplitude response.**—Since oriented cellulose molecules exhibited strong parallel dichroism, we performed 2D FT-IR with light polarized parallel to an applied small amplitude (100  $\mu$ m) oscillation. Dynamic spectra were collected from wet samples pre-stretched to 21% strain. The dynamic spectra of **C**, **CP**, and **CXG** were only considered in the 1200–900  $\text{cm}^{-1}$  region because no dynamic response was observed in the region 1800–1200  $\text{cm}^{-1}$  or below 900  $\text{cm}^{-1}$ . The IP spectrum was more intense than the Q spectrum in response to the applied small

amplitude (100  $\mu\text{m}$ ) sinusoidal displacement at 20 Hz frequency (i.e., **C** on Fig. 4(a)).

Two-dimensional correlation spectra<sup>13,20</sup> were examined in order to decide whether the network biopolymers were independent, since in synthetic polymer blends<sup>19</sup> such spectra have been shown to provide sub-molecular-level insight into the interactions between specific functional groups. The synchronous 2D cross-peak values for the studied samples are listed in Table 3. **C** (Fig. 5(a)) gave cross peaks at 1162, 1112, 1062, and 1030  $\text{cm}^{-1}$  (assignment see Table 2), representing similar time-dependent movements of specific cellulose groups. **CP** (Fig. 5(b)) was essentially the same as for **C** and our data showed no evidence of connected motion between the two networks in the **CP** composite, consis-

tent with earlier evidence.<sup>4</sup> The dynamic spectra of the **CXG** exhibited bands at 1162 and 1080  $\text{cm}^{-1}$  in IP spectrum (not shown). In the 2D correlation maps (Table 3, Fig. 5(c)) the intense cellulose and xyloglucan cross-peaks appearing at the off-diagonal positions at 1162 and 1080  $\text{cm}^{-1}$  indicated a strong synchronous correlation between cellulose and xyloglucan (Table 3), thus providing evidence that the two macromolecules move collectively, as suggested earlier.<sup>3</sup> These cross-peaks are the same as in the completely parallel oriented dry spruce-pulp cellulose<sup>12</sup> model.

Spectra of completely oriented cellulose sheets made of spruce pulp had shown<sup>12</sup> the band at 1064  $\text{cm}^{-1}$  with a shoulder at 1076  $\text{cm}^{-1}$  in parallel orientation. However, in the case of partially oriented **CXG**, the

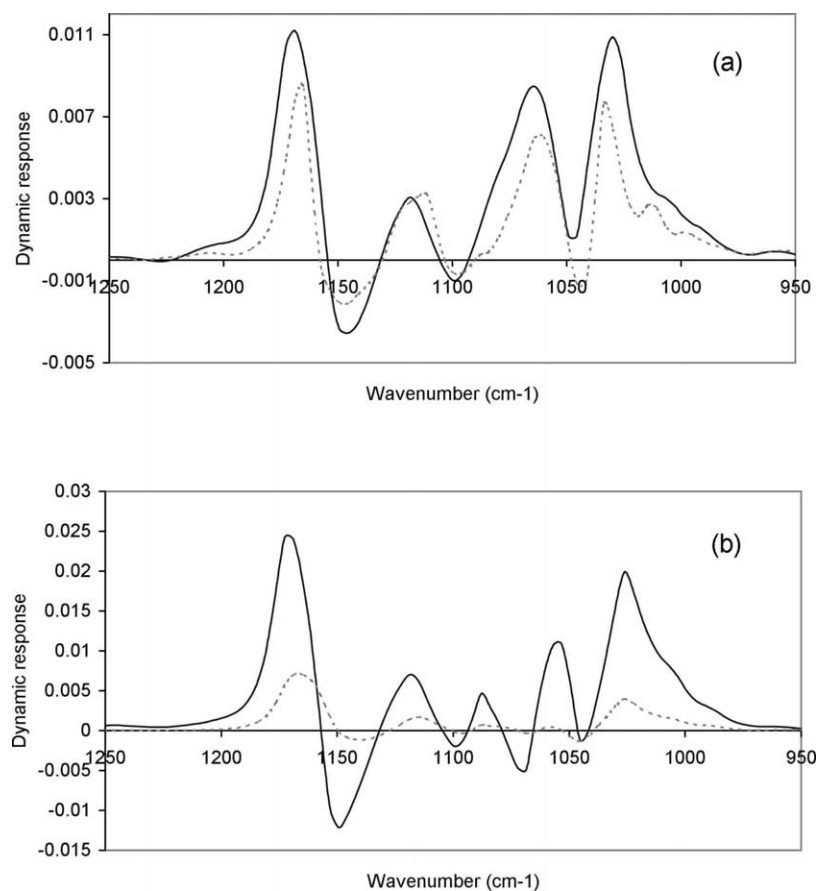


Fig. 4. Dynamic IP (—), and Q (---) spectra of **C** measured at sample modulation frequency (SMF) of: 20 Hz (a) and 5 Hz (b). Sample modulation amplitude = 100  $\mu\text{m}$ .

Table 3

2D FT-IR cross-peaks as observed in 21% pre-stretched cellulose composites at 20 Hz SMF

Sample	Wavenumbers ( $\text{cm}^{-1}$ )					
<b>C</b>	1162–1057	1115		1062–1055		1037–1025
<b>CP</b>	1170–1057	1115		1057		1030
<b>CXG</b>	1060	1115	1080–1070	1065–1055	1040	1035–1025

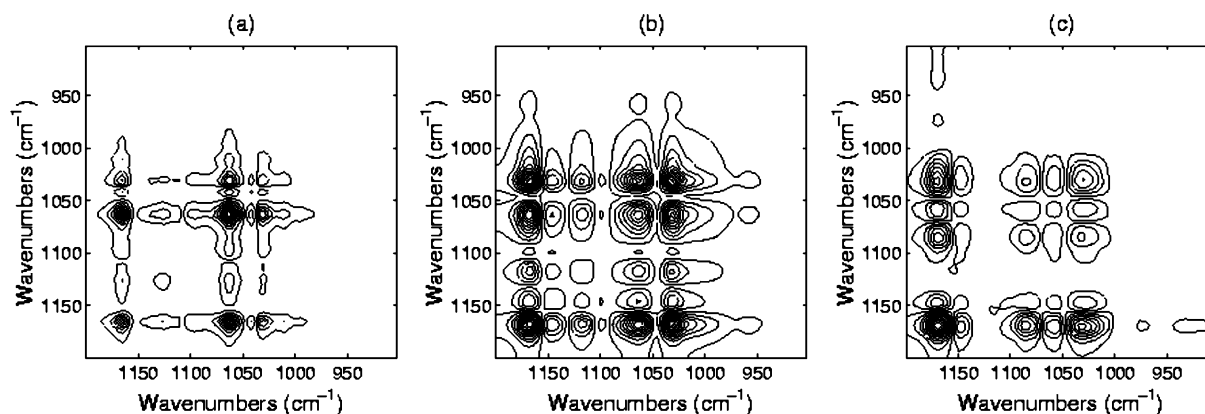


Fig. 5. 2D FT-IR synchronous correlation maps of **C** (a), **CP** (b) and **CXG** (c) measured at sample modulation frequency (SMF) of 20 Hz. Sample modulation amplitude = 100  $\mu\text{m}$ .

1080  $\text{cm}^{-1}$  band is a clearly defined peak and together with the 1040  $\text{cm}^{-1}$  band, already shown in the linear stretching experiment, they are assigned to the xyloglucan contribution.

These results are also in agreement with those from onion epidermis.<sup>13</sup> Wide-angle X-ray scattering (WAXS) has also shown that pectin does not bind to the cellulose whereas xyloglucan binds strongly to cellulose.<sup>24</sup>

*Sample modulation at different frequencies.*—The w- and m-samples were measured at 5, 10, 16, 20, 25, and 50 Hz SMF. The dynamic IP and Q spectra were well resolved at 5–25 Hz in contrast to 50 Hz, where the signal to noise ratio was very low and the spectra gave no information about any response to the applied strain. This observation suggests that the molecular interaction may depend on the mechanical frequency and at high frequencies the motions in cellulose composites lose coherence. At low frequencies (5, 10 Hz, Fig. 4(b)), the intensity of the Q spectra was small relative to IP spectra in **CP** and **CXG**, showing that the polymers responded almost synchronously to the applied strain indicating an elastic response of the composite networks to the applied small amplitude (100  $\mu\text{m}$ ) oscillation. It is interesting that earlier small deformation rheology of these systems showed  $E' > E''$ , also indicating a dominance of the elastic over the viscous response.<sup>3,4</sup> The intensity of Q spectra increased at higher frequencies (i.e., 20 Hz, Fig. 4) consistent with a loss of synchronicity.

Cross peaks arising from the four cellulose groups were seen at all oscillation frequencies in **C** and **CP**. In **CXG**, xyloglucan and cellulose resulted in cross-peaks at 5–20 Hz but the 1120  $\text{cm}^{-1}$  cellulose peak was weak or absent suggesting a changed cellulose geometry at the O-2···O-6–H hydrogen bond in the presence of xyloglucan. The presence of the xyloglucan 1070  $\text{cm}^{-1}$  peak at low frequencies showed that stress transmission occurred in both cellulose and hemicellulose. At 25 Hz,

cross peaks at 1030 and 1165  $\text{cm}^{-1}$  suggest that the cellulose glycosidic and the C-6–H-2–O-6–H side groups interact at high frequencies. The results suggest that dynamic 2D FT-IR data can be linked to the viscous and elastic rheological properties of biopolymers.

The results show that 1D FT-IR and dynamic 2D FT-IR spectroscopies can be used together or independently to characterize biopolymer systems depending on physical conditions, and are prospective in biological-research applications on a microscopic scale. Cellulose, pectin, and xyloglucan are major constituents of the plant cell wall and interactions within and between them shown by FT-IR spectroscopy are crucial in understanding the structure of the plant cell wall.

## Acknowledgements

This work was funded by a BBSRC competitive strategic grant. The authors gratefully acknowledge Dr E. Chanliaud (Unilever) for sample preparation, Dr N. Wellner (IFR) for technical advice with dynamic 2D FT-IR, Dr M.C. McCann (JIC, Norwich) and Dr K.W. Waldron (IFR) for helpful discussion.

## References

1. Chandrasekaran R. *Adv. Carbohydr. Chem. Biochem.* **1997**, 52, 311–439.
2. Whitney S. E. C.; Brigham J. E.; Darke A. H.; Reid J. S. G.; Gidley M. J. *Plant J.* **1995**, 8, 491–504.
3. Whitney S. E. C.; Gothard M. G. E.; Mitchell J. T.; Gidley M. J. *Plant Phys* **1999**, 121, 657–663.
4. Chanliaud E.; Gidley M. J. *Plant J.* **1999**, 20, 25–35.
5. Liang, C. Y.; Marchessault, R. H. *J. Polym. Sci.* **1959**, 37, 385–395; *J. Polym. Sci.* **1959**, 37, 269–278.
6. Marchessault R. H.; Sundararajan P. R. *Cellulose. In The Polysaccharides*; Aspinall G. O., Ed.; Academic Press: New York, 1983; Vol. 2.



7. Sugiyama J.; Persson J.; Chanzy H. *Macromolecules* **1991**, *24*, 2461–2466.
8. Marechal Y.; Chanzy H. *J. Mol. Struct.* **2000**, *523*, 183–196.
9. Siesler H. W.; Zebger I.; Kulinna Ch.; Okretic S.; Shilov S.; Hoffmann U. In *Modern Polymer Spectroscopy*; Zerbi G., Ed.; Wiley-VCH: Weinheim, 1999; pp 33–86.
10. Hinterstoisser B.; Salmen L. *Cellulose* **1999**, *6*, 251–263.
11. Hinterstoisser B.; Salmen L. *Vibr. Spectr.* **2000**, *22*, 111–118.
12. Hinterstoisser B.; Åkerholm M.; Salmen L. *Carbohydr. Res.* **2001**, *334*, 27–37.
13. Wilson R. H.; Smith A. C.; Kačuráková M.; Saunders P. K.; Wellner N.; Waldron K. W. *Plant Phys* **2000**, *124*, 397–405.
14. Besbes S.; Bokobza L.; Monniere L.; Bahar I.; Erman B. *Polymer* **1993**, *34*, 1179–1182.
15. Griffiths P. R.; de Haseth J. A. *Fourier Transform Infrared Spectrometry*; Chemical Analysis: New York, 1986; pp 437–450.
16. Koenig J. L. *Spectroscopy of Polymers*; Elsevier: Amsterdam, 1999; pp 147–206 Chapter 4.
17. Wilkes G. L.; Stein R. S. In *Structure and Properties of Oriented Polymers*; Ward I. M., Ed.; Chapman and Hall: London, 2000 Chapter 2.
18. Graff D. K.; Haochuan W.; Palmer R. A.; Schoonover J. R. *Macromolecules* **1999**, *32*, 7147–7155.
19. Marcott C.; Dowrey A. E.; Noda I. *Anal. Chem.* **1994**, *66*, 1065–1075.
20. Noda I.; Dowrey A. E.; Marcott C. In *Modern Polymer Spectroscopy*; Zerbi G., Ed.; Wiley-VCH: Weinheim, 1999; pp 1–32.
21. Wellner N.; Kačuráková M.; Malovíková A.; Wilson R. H.; Belton P. S. *Carbohydr. Res.* **1998**, *308*, 123–131.
22. Kačuráková M.; Capek P.; Sasinkova V.; Wellner N.; Ebringerova A. *Carbohydr. Polym.* **2000**, *43*, 195–203.
23. Kataoka Y.; Kondo T. *Macromolecules* **1998**, *31*, 760–764.
24. Astley O. M.; Donald A. M.; Chanliaud E.; Whitney S. E. C.; Gidley M. J. *SRS Sci. Rep.* **2000**, 114–145.
25. Voyiatzis G. A.; Andrikopoulos K. S.; Papatheodorou G. N.; Kamitsos E. I.; Chrissikos G. D.; Kapoutsis J. A.; Anastasiadis S. H.; Fytas G. *Macromolecules* **2000**, *33*, 5613–5623.
26. Astley, O. M.; Chanliaud, E.; Donald, A. M.; Gidley, M. J. submitted.